Maintaining Awareness of the Focus of Attention of a Conversation: A Robot-Centric Reinforcement Learning Approach

Marynel Vázquez[1], Aaron Steinfeld[1] and Scott E. Hudson[2,3]

***Abstract*— We explore online reinforcement learning techniques to find good policies to control the orientation of a mobile robot during social group conversations. In this scenario, we assume that the correct behavior for the robot should convey attentiveness to the focus of attention of the conversation. Thus, the robot should turn towards the speaker. Our results from tests in a simulated environment show that a new state representation that we designed for this problem can be used to find good policies for the robot. These policies can generalize across interactions with different numbers of people and can handle various levels of sensing noise.**

I. INTRODUCTION

Mobile social robots are being designed to operate in human environments, with and around groups of people. For example, Cobots [1] navigate university buildings and perform tasks in collaboration with nearby users. Frog [2] has operated as a museum tour guide, often guiding groups of visitors from one place to another. Even though these and other projects within the robotics community have improved robot capabilities in human environments, autonomous robot motion during group conversations has been understudied. Most efforts to control the spatial behavior of robots in these situations have relied on tele-operation [3], [4], [5]. A few exceptions are rule-based approaches [6], which tend to generalize poorly to new situations, and generative models of proxemic behavior [7]. The latter models worked for adapting a robot's position with respect to a single user, but have not been tested with more people.

Inspired by the success of reinforcement learning (RL) in robotics [8], we explore RL techniques to find good policies to control the orientation of a robot during social group conversations. Body orientation is important because it is often considered as communicative and meaningful by users [9]. For robots with a small number of degrees of freedom, like Cobot [1] or Frog [2], body orientation controls the direction of important social features, such as their faces, as well as the directions of many of their sensors. Thus, their orientation can significantly affect users' interpretations of their actions and their sensing capabilities. Furthermore, body orientation can be used to induce spatial reconfigurations during interactions [10]. This is a subtle and effective strategy for redirecting the focus of a conversation.

We approach the problem of controlling the orientation of a robot during group conversations using the Oz of Wizard methodology [11]. Our efforts are focused on evaluating RL approaches in simulated group conversations (Fig. 1) as a precursor to future work with real users. The simulation offers the opportunity to systematically study the effect of sensing noise on the performance of the robot as well as the generalization of learned policies to other group interactions. This is a first step towards automatically optimizing robots' spatial behavior during situated conversations with users and reducing the amount of engineering required for this task.

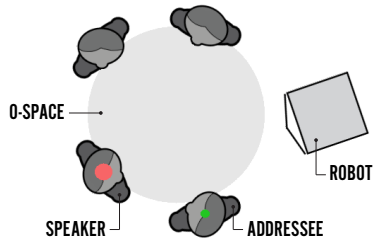

Fig. 1. Simulated group conversation between a robot and four people. The red and green circles on top of the agents identify the speaker and addressees, respectively. The big gray circle represents the o-space of the group's F-formation.

One of our main contributions is a robot-centric state representation for reinforcement learning that is agnostic to the number of people in the conversation. This means that the same representation can be used to control the robot while it interacts with 2, 3, 4 or more people and that the learned policies can easily generalize across these scenarios.

Even though robots may take a turn to speak during conversations, we concentrate our evaluation on situations in which the users are the active speakers and the focus of attention. These situations are interesting to study from a control perspective because the robot does not have control of the interaction dynamics in them and, thus, must adapt to the flow of the conversation. Under these circumstances, we assume that the correct behavior for the robot is to turn towards the speaker to convey attentiveness to this person and maintain awareness of the focus of attention.

The rest of this paper is organized as follows. Section II describes our general approach to control the orientation of a robot with reinforcement learning. Section III presents background models from social psychology that informed the design of our simulation environment and details the interaction dynamics and sensing mechanisms that we modeled for this work. Section V and VI then describe our empirical evaluation and results. Finally, Section VII discusses the limitations of our work and the implications of our findings.

[1] Robotics Institute, Carnegie Mellon University, Pittsburgh, PA. {marynel, steinfeld}@cmu.edu

[2] Human-Computer Interaction Institute, Carnegie Mellon Univerity, Pittsburgh, PA. scott.e.hudson@cs.cmu.edu

[3] Disney Research, Pittsburgh, PA.

II. GENERAL APPROACH

We model our motion control problem as a sequential decision-making process. At any time-step t, the robot (or agent) receives some representation of the environment *state* $\mathbf{s}_t$ and executes an *action* a_t. Executing this action triggers a transition to a following state, represented by $\mathbf{s}_{t+1}$, and results in an immediate *reward* r_{t+1}. The goal of the robot is to choose actions that maximize the discounted total reward that it receives while it interacts with the world. That is, maximize $\sum_{t=0}^{\infty} \lambda^t r_{t+1}$ with $\lambda \in [0, 1]$ a discount rate.

Out of the many RL techniques that exist, we focus on evaluating popular online approaches that estimate an *action-value function* $Q(\mathbf{s}, a)$ to try to find solutions to the motion control problem. The function

$$Q^{\pi}(\mathbf{s}, a) = E_{\pi}\left[\sum_{k=0}^{\infty} \gamma^k r_{t+1+k} | \mathbf{s}_t = \mathbf{s}, a_t = a\right]$$

is an estimate of how good it is to choose action a in a given state $\mathbf{s}$ and then follow policy π. Readers interested in more details about this function are encouraged to refer to [12].

Online approaches are advantageous for our task because they improve as the robot interacts with people and they can adapt quickly to specific interaction dynamics. The latter is particularly advantageous when the social context changes, e.g., when some of the members of the conversation leave or others join the interaction.

III. GROUP SIMULATION

We developed a simulated environment to test control policies for a robot. The simulation was inspired by models from social psychology that explain human spatial behavior during free-standing group conversations [13], [14].

A. Background

When people stand freely in open, public spaces, they tend to maintain distinct spatial organizations known as face formations, or *F-formations* in short. F-formations maximize the opportunities of the interactants to monitor one another during a conversation and maintains their group as a spatially distinct unit from other nearby interactions.

Face formations begin when the members of a group position themselves such that their *transactional segments* intersect (Fig. 2a). These segments extend in front of each person and encompass the physical space that they are using for their current activity.

For group conversations, the intersection of the transactional segments is known as the *o-space* of the corresponding F-formation. In the case of pairs, the o-space is between the members of a face-to-face arrangement (as in Fig. 2a) or in front of them in a side-by-side or "L" arrangement (Fig. 2b and 2c). This pattern can also be observed for bigger groups, which tend to form semi-circular or circular arrangements (Fig. 2d and 2e). Experimental evidence suggests that the notion of transactional segments and o-spaces can be applied to social robots as well [14], [10]. Figure 1 provides an example in the context of our simulation.

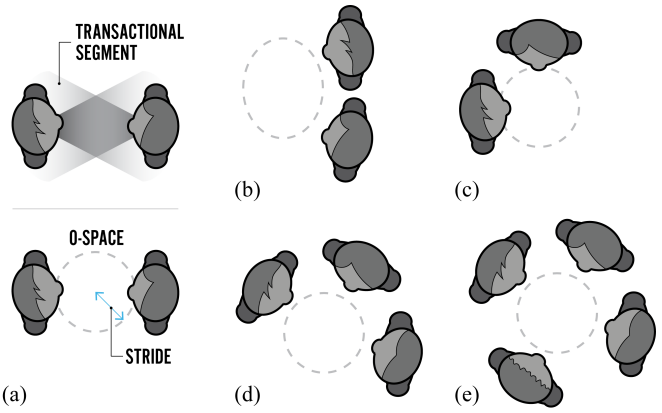

Fig. 2. Various spatial arrangements that may appear during human conversations. The top sketch in (a) shows the transactional segments of two people. The intersection of these segments is known as the o-space (dashed circles). The bottom sketch in (a) indicates the stride of the o-space, which is one of the main parameters of our simulation (see Sec. III-C).

B. Main Loop

Our simulation modeled a free-standing group conversation with an established F-formation. To start, the simulation placed the interactants in a circular arrangement and randomly chose the first speaker and the addressee(s) (either one person or the whole the group). The simulation then repeated the steps below:

1) Update the simulated clock.
2) Update the state of the robot with the latest action that was chosen by the RL agent that controls it.
3) Choose new speaker and addressee if the previous speaker finished talking.
   a) Set desired head orientation for the speaker.
   b) Set desired head orientation for the people who are listening.
4) Update the states of all the people in the conversation.
5) Compute the reward for the robot.
6) Update the robot's internal representation of the state of the conversation based on its sensing capabilities.
7) Return the reward and new state representation to the RL agent so that it can choose the next action.

The set of actions that the robot could execute were angular velocity commands that changed its orientation with respect to the group. The robot's representation of the state of the conversation is later described in Sec. IV.

In terms of head orientations, speakers turned their heads towards their addressee or towards the center of the o-space if they spoke to the whole group. The other people in the conversation turned their heads towards the speaker, as described in the next section. In general, heads rotated at a fixed angular velocity towards their respective target, typically during multiple simulation steps.

For this work, we never allowed the robot to take a turn to speak. As a result, it had to adapt to the flow of the conversation set by the rest of the group.

C. Main Simulation Parameters

The main parameters that controlled the spatial arrangement of the group and the dynamics of the interaction were:

Number of interactants: The number of people in the conversation, including the robot.

O-space center: The location of the center of the o-space in the world-coordinate frame of the simulation.

Stride: The expected distance between the center of the o-space and the interactants (as depicted in Fig. 2a).

Time step: Time elapsed between simulation updates.

Robot actions: List of angular velocity commands that could be executed by the robot. In particular, we used the set $[-15.0, -7.5, 0.0, 7.5, 15.0]$ (in deg/sec) for this work.

Speaking time distribution: Normal distribution that modeled how long a person typically spoke for. In general, we used $\mathcal{N}(5.0, 2.0)$, but prevented sampled values from being smaller than 0.5 secs to avoid very short speaking times.[1]

Look-at noise: When a person i in the simulation looked at the speaker, his or her head was set towards the angle β_i:

$$\beta_i = \arctan(d_y/d_x) + \varepsilon_i \text{ with } \varepsilon_i \sim \mathcal{N}(0, \sigma_i^2) \quad (1)$$

where $\mathbf{d} = [d_x \ d_y]^T$ denotes the direction towards the speaker from person i. The noise term ε_i in eq. (1) controlled how accurately the person looked at the speaker, depending on the standard deviation σ_i. Note that when σ_i made the head turn more than 90 degrees from the front of the person, we clamped β_i to prevent the head from turning backwards.

D. Robot Perception

We modeled the robot as a platform with a small number of degrees of freedom, similar to Cobot [1] or Frog [2]. The robot had a camera and a microphone array fixed to the front of its body. The camera could be used to detect the position of people, as well as their head and body orientations. The microphone array provided the angular directions toward nearby speakers from the robot's perspective.

The sensors had configurable fields of view. People within these fields of view could be sensed with some probability; those outside were not detected at all. The specific values that we used for these parameters are provided in Sec. VI.

E. Reward

In this work, we assumed that the correct behavior for the robot was to turn towards the speaker. Consequently, the reward r_{t+1} that the environment provided to the robot for taking an action a_t was:

$$r_{t+1} = \exp(-\varphi^2) + b \quad (2)$$
$$\text{with } b = \begin{cases} 1 & \text{if } \text{abs}(\varphi) <= \tau \text{ and } a_t == 0.0 \\ 0 & \text{otherwise} \end{cases}$$

[1]We acknowledge that this model is a crude approximation of real group conversations because people often speak for significantly longer than 5 secs. We opted for short speaking times, though, because longer speeches simplify the control problem by reducing the number of speakers in any given interaction.

The angle $\varphi \in [-\pi, \pi]$ was the difference between the orientation of the robot and the angle representing the direction towards the speaker from the robot's position. The bonus b was given to reward zero angular velocity commands when the difference φ was small. In general, we used 10 degrees for τ to prevent oscillatory motions.

F. Limitations

Even though the simulation was useful to explore reinforcement learning techniques for motion control, it is by no means a perfect model of the real world. Our simulation did not capture all the complexity and variability of human behavior during group conversations nor sensing noise. Nonetheless, our efforts are an important first step towards testing RL techniques for the problem under consideration. The policies learned from our simulation can be considered as prior knowledge for learning better behaviors with real users. Furthermore, the simulation allowed us to explore the sensitivity of several methods to particular types of noise, something that is hard to accomplish during human-robot interaction experiments [11].

IV. STATE REPRESENTATION

Our key contribution in this work is a state representation that is well suited to solve our motion control problem with RL techniques. This representation was composed of six features:

f1. Continuous feature in $[-\pi, \pi]$ representing the rotation that the robot needed to execute to direct its body towards the speaker. This value is the same as φ in eq. (2) if the speaker was within the field of view of the robot's microphone array and the sensor detected the audio signal coming from this person. Otherwise, *f1* was set to zero by convention.

f2. Binary feature indicating if *f1* is valid or not. This feature was zero when no audio signal was detected by the microphone array; otherwise, *f2* was one.

f3. Continuous feature in $[-\pi, \pi]$ representing the rotation that the robot needed to execute to direct its body towards the location of maximum *social saliency* induced by the visible people in its group. Social saliency encoded gaze concurrences and was estimated using the primary gaze rays of the people detected by the robot's camera, as described in [15] and illustrated in Fig. 3. When multiple locations were socially salient and had equal contribution from the primary gaze rays of the visible people, ties were broken randomly and only one location was used to compute *f3*. When a single person was detected by the camera and no gaze concurrence could be computed, we uniformly sampled possible social saliency locations along the primary gaze ray of this person and used their average for *f3*. If nobody was visible, then *f3* was set to zero by convention.

f4. Binary feature indicating if *f3* is valid. This feature was zero if nobody was detected through the robot's camera and, thus, social saliency could not be computed. Otherwise, *f4* was set to one.

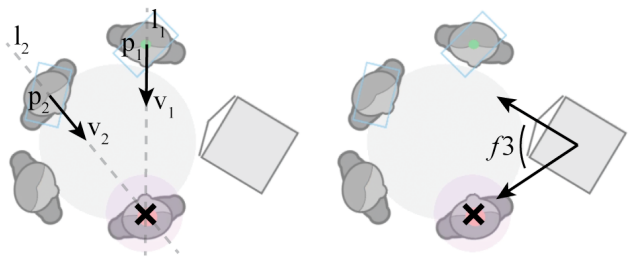

Fig. 3. Example of the primary gaze rays ($\mathbf{l_1}$ and $\mathbf{l_2}$) used to compute the point of maximum social saliency (a) and the resulting feature *f3* used in our state representation (b). The point of maximum social saliency is marked with an $\times$ and surrounded by a light-colored circle. The primary gaze rays were estimated only for persons 1 and 2, who were visible through the robot's cameras. These rays were estimated based on the position and head direction ($\mathbf{v}$) of each person.

f5. Continuous feature in $[-\pi, \pi]$ representing the rotation that the robot needed to execute to orient its body towards the center of the o-space of its conversational group. We computed an estimate $\mathbf{c}$ of the true o-space location using an exponential moving average of center proposals:

$$\mathbf{c} = (1.0 - n * a)\mathbf{c} + a \sum_{i=1}^{n} \underbrace{\mathbf{p}_i + s * \mathbf{u}_i}_{\text{center proposal}} \tag{3}$$

where $a \in [0, 1]$ controlled the contribution of every proposal, s was an expected value for the stride of the o-space, n was the total number of people visible through the robot's camera, $\mathbf{p}_i$ was the position of the i-th person that was visible, and $\mathbf{u}_i$ was a unitary vector pointed in the same direction as the front of the body of person i. The model used to generate o-space center proposals ($\mathbf{p} + s * \mathbf{u}$) was inspired by prior work [16], [17] and was used to initialize $\mathbf{c}$ with the proposal corresponding to the first person detected by the robot when the simulation started. Before any person was detected, *f5* was zero by convention.

f6. Binary feature indicating if *f5* is valid. If no o-space center had been estimated, then *f6* was zero. Otherwise, *f6* was one.

A. Properties

Our state representation is agnostic to the size of the group. This means that the same features can be used to describe conversations with a few people or with more interactants.

Because the features are computed from the perspective of the robot, their descriptive power depends on the performance of the robot's sensors. For example, the more people are detected at any given time, the more the estimate of the o-space center converges to the true value. The more people are detected, the closer the point of maximum social saliency is to the place where most gaze directions converge. This place is typically the location of the speaker.

V. EVALUATION

We performed a series of experiments to evaluate several RL agents in our simulated environment. Our goal was not to prove the superiority of one method, but rather to evaluate empirically what kind of approach may be better suited for our particular task and whether the proposed state representation generalized as expected. More precisely, our experiments focused on addressing:

1) whether a robot could quickly learn reasonable policies for the orientation task in our simulated environment;
2) how the performance of the RL agents under consideration degraded with noisy measurements;
3) how their performance could be affected by atypical human behavior; and
4) whether learned policies could generalize to conversations with more or fewer interactants.

To address the first goal above, we studied the amount of reward that several agents received as a function of time, as well as how quickly their performance saturated. This test included agents that estimated action values for discrete versions of the state space or that approximated them using linear regression. For the second and third goals, we studied how measurement noise and variability in human motion affected the performance of the agents that, on average, learned good policies faster. For the last goal, we tested policies that were learned from interacting with 4 people in other group conversations.

A. Agents

We considered several agents for our evaluation. First, we decided to test model-based RL methods because they tend to be more sample efficient than model-free approaches when good transition and reward models can be learned quickly. These methods included TEXPLORE [18], which was designed for the robotics domain, and DYNA-2 [19], which can leverage prior experience while learning. Because the latter architecture uses Sarsa [12] to estimate the action-value function Q, then we also decided to test Sarsa by itself as a model-free method. Brief descriptions of the specific versions of the agents that we considered in our evaluation are provided below for completeness.

Sarsa(λ): Baseline on-policy learning agent [12]. This implementation discretizes the continuous features of the state space (Sec. IV) and estimates the action-value function Q using a tabular representation. With any new tuple $(\mathbf{s}_t, a_t, r_t, \mathbf{s}_{t+1}, a_{t+1})$,

$$\begin{aligned} Q_{t+1}(\mathbf{s}, a) &= Q_t(\mathbf{s}, a) + \alpha \delta_t e_t \text{ for all } (\mathbf{s}, a) \\ \text{with } \delta_t &= r_{t+1} + \gamma Q_t(\mathbf{s}_{t+1}, a_{t+1}) - Q_t(\mathbf{s}_t, a_t) \end{aligned} \tag{4}$$

where α is the learning rate, γ is the discount factor, and e_t is the (accumulating) eligibility trace [20]:

$$e_t = \begin{cases} \gamma\lambda e_{t-1} + 1 & \text{for } (\mathbf{s}_t, a_t) \\ \gamma\lambda e_{t-1} & \text{for all other state-action pairs} \end{cases} \tag{5}$$

which represents the credit assigned to state-action pairs for subsequent errors in evaluation.

For action selection, this agent uses the common ϵ-greedy policy, which chooses the best actions $\arg\max_a Q(\mathbf{s}, a)$ with a probability of $1 - \epsilon$. Otherwise, it selects a random action.

Sarsa(λ) with tile coding and adaptive learning rate: Sarsa agent with linear function approximation [21]:

$$Q(\mathbf{s}, a) = \phi(\mathbf{s}, a)^T \theta \tag{6}$$

where ϕ is a function that transforms the state-action pair to a large binary vector with tile coding [22] and θ is a collection of weights. The weights get updated by the rule $\theta_{t+1} = \theta_t + \alpha\delta_t e_t$, with the eligibility traces being $e_t = \gamma\lambda e_{t-1} + \phi(\mathbf{s}_t, a_t)$ and α being updated automatically according to [23]. This agent also uses an ϵ-greedy policy.

DYNA-2: RL architecture that combines sample-base learning with sample-based planning [19], as described in Algorithm 1. The agent has two "memories" that encapsulate all of the features and parameters used to estimate the value function. The *permanent* memory (ϕ, θ) is updated from real-world experiences and is used to compute the best overall estimate of the action-value function $Q(\mathbf{s}, a) = \phi(\mathbf{s}, a)^T\theta$ ("learn" procedure of Alg. 1). The *transient* memory $(\bar{\phi}, \bar{\theta})$ is updated during simulations to track a local correction to the permanent memory ("search" procedure). This update is achieved with the combined action-value function $\bar{Q}(\mathbf{s}, a) = \phi(\mathbf{s}, a)^T\theta + \bar{\phi}(\mathbf{s}, a)^T\bar{\theta}$.

Algorithm 1: Main steps of DYNA-2

Procedure learn *($\mathbf{s}_t$, a_t, r_t, $\mathbf{s'}_{t+1}$)*
- Store ($\mathbf{s}_t$,a_t,r_t,$\mathbf{s}_{t+1}$) to update dynamics model
- search ($\mathbf{s}_{t+1}$) and pick next action $a_{t+1} = \pi(\mathbf{s}, \bar{Q})$
- `// update permanent memory (Sarsa)`
- $\theta_{t+1} = \theta_t + \alpha[r_t + \gamma Q(\mathbf{s}_{t+1}, a_{t+1}) - Q(\mathbf{s}_t, a_t)]e_t$
- **return** (a_{t+1})

Procedure search *(**s**)*
- **for** $k = 1$ **to** $num\_rollouts$ **do**
  - Initialize $\bar{e}_0 = \mathbf{0}$ and $\mathbf{s}_0 = \mathbf{s}$
  - Pick action $a_0 = \bar{\pi}(\mathbf{s}_0, \bar{Q})$
  - **for** $t = 0$ **to** $max\_steps - 1$ **do**
    - $(\mathbf{s}_{t+1}, r_t) =$ queryDynamicsModel$(\mathbf{s}_t, a_t)$
    - Pick next action $a_{t+1} = \bar{\pi}(\mathbf{s}_{t+1}, \bar{Q})$
    - `// update transient memory`
    - $\bar{\theta}_{t+1} = \bar{\theta}_t + \bar{\alpha}[r_t + \gamma\bar{Q}(\mathbf{s}_{t+1}, a_{t+1}) - \bar{Q}(\mathbf{s}_t, a_t)]\bar{e}_t$

The main difference between Alg. 1 and its description by Silver and colleagues [19] is that we apply DYNA-2 to a non-episodic scenario with discounted returns ($\gamma < 1$). Moreover, we use Sarsa(λ) with tile coding and an adaptive learning rate to estimate θ and $\bar{\theta}$. For the transition and reward models, we use regression forests, as described in the next paragraphs for TEXPLORE. Whenever enough samples are collected to learn a new model, we clear DYNA's transient memory so that it quickly adapts to the new dynamics.

TEXPLORE: Model-based architecture that uses sample-based planning [18]. In particular, this architecture uses a regression forest to estimate the transition and reward functions from real experience. Every time a query is made for planning, a random tree from the forest is chosen to make the prediction. This tree can be considered as one possible hypothesis of the true model of the domain. For planning, this architecture uses the UCT(λ) algorithm with discretized states-action spaces. Sample actions are selectively chosen using Upper Confidence Bounds [24].

In contrast with the original description of TEXPLORE [18], our implementation does not generalize action-values across depths in the search tree nor runs the act, plan, and model threads in parallel. The first modification was made because generalizing values resulted in poor performance in our particular domain. The second change simplified our implementation. Even though speed is important for robotics applications, such as ours, it was not a crucial factor for the present work.

B. Other Implementation Details

We used RL-Glue[2] as the interface between our simulated environment with the agents under consideration. For the Sarsa(λ) agent with tile coding, we used PyRL's implementation.[3] For the rest, we used our own implementation in Python, as described in the previous section. Moreover, we used the same model approximator for Dyna-2 and TEXPLORE. The approximator was a collection of independent regression forests for each of the dimensions of the state space and for the reward function, as proposed by Hester [18]. Our code extended the functionalities of the regression forest model of the Scikit Learn library[4] with an option to query the prediction of a randomly-chosen tree in the forest.

VI. RESULTS

Unless otherwise noted, the results presented in this section are averages over 10 runs of 18000 steps (equivalent to 1 hour of interaction time) and actions were executed every 0.2 seconds. We set the field of view and detection probability of the microphone array on the robot to 100 degrees and 0.9, respectively. For the camera, we used 80 degrees and 0.75. These values were set based on our prior experience with off-the-shelf sensors of this kind.

The simulations had a total of 5 interactants (including the robot) which were arranged in a circular formation with a stride of 1.25 meters, as illustrated in Fig. 1. In general, future rewards were discounted with $\gamma = 0.7$.

Whenever the state space was discretized by an agent, we used 24 bins for each of the continuous angular features. For Sarsa(λ) and the ϵ-greedy policies, we set $\lambda = 0.4$ and $\epsilon = 0.1$, respectively. For the discrete Sarsa agent, $\alpha = 0.7$; for the continuous version, we used 64 tiles to approximate the Q function. In the case of DYNA-2 and TEXPLORE, we used regression forests with 15 trees to estimate a model of the dynamics. This model was updated every 300 samples (i.e., once a minute). For sample-based planning, we used 16 rollouts with 3 look-ahead actions. These parameters provided good results in our simulated environment.

[2] `http://glue.rl-community.org`
[3] `https://github.com/amarack/python-rl`
[4] `http://scikit-learn.org`

A. Learning to Orient

First, we studied how quickly the RL agents under consideration learned to orient towards the speaker. We considered the same look-at noise distribution $\mathcal{N}(0, \sigma^2)$ in eq. (1) for all the people in the simulation, where σ was set to $0.0, 0.3, 0.6, 0.9$, or 1.2 radians (which is equivalent to 0.0, 17.2, 34.3, 51.5, and 68.8 degrees). In the particular case where $\sigma = 0$, no noise was added to the head orientations.

In general, all the agents converged to good policies within 1000 to 2000 steps (i.e., within 3.3 to 6.6 minutes) except for the baseline version of Sarsa with a tabular Q representation. The poor performance of this version of Sarsa with respect to the other agents can also be observed in Figure 4. This plot shows the number of speakers towards whom the robot failed to orient with an angular velocity of 0.0 rad/sec and with $abs(\varphi)$ in eq. (2) less than 10 deg. These can be considered speakers the the robot failed to acknowledge properly. The fact that all the agents but the baseline version of Sarsa found good policies quickly suggests that generalizing Q estimates across states is beneficial for our task.

Figure 5 shows the proportion of steps in which the agents achieved good behavior and received a bonus $b = 1.0$ as part of their reward (see eq. (2)). In general, model-based agents performed the best in terms of orienting properly towards the speakers. This result reinforces the idea that random forests are sample efficient when it comes to estimating dynamics models [18]. Furthermore, Fig.5 shows that the more people look away from the speaker, the worse the agents tend to perform. This reduction in performance happens because higher σ values lead to fewer gaze concurrences, which is precisely what social saliency tries to estimate. One option to counter-act this effect is to estimate σ for every person during the conversation and incorporate this information into the estimate of social saliency (see Section 3.2 of [15]).

Figure 6 shows the cumulative reward that the agents obtained during the 18000 steps of interaction time. TEXPLORE clearly outperformed the other agents in this respect, likely because of its better policy in comparison to ϵ-greedy.

B. Sensitivity to the Detection Probabilities

Because multiple factors can affect robot perception, such as background audio or illumination, we decided to further investigate how different detection probabilities for the robot's sensors affected its performance. In particular, we focused on evaluating DYNA-2 and TEXPLORE in this experiment, given that they performed the best previously.

We evaluated two detection probabilities for the microphone array (0.75 and 0.90) and three for the camera (0.60, 0.75 and 0.90). As before, this experiment was repeated 10 times per agent until it completed 18000 steps. We used $\mathcal{N}(0, 0.6^2)$ for the look-at noise distribution of all the people.

Figure 7 shows the proportion of steps in which the robot received a positive reward with the different detection probabilities. The results were affected by the detection probability of the microphone array: the lower the probability, the fewer times the robot received a positive bonus. Interestingly, the results did not vary much with lower detection probabilities for the camera.

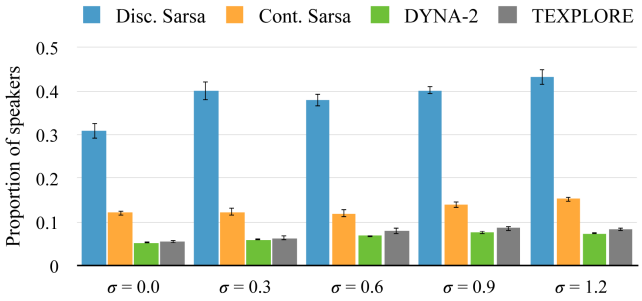

Fig. 4. Proportion of speakers towards whom the agents failed to orient as a function of the look-at noise (lower is better). "Disc. Sarsa" is the discrete version of Sarsa(λ) with tabular Q; "Cont. Sarsa" is the continuous version with tile coding. Error bars represent standard errors. (Best viewed in color)

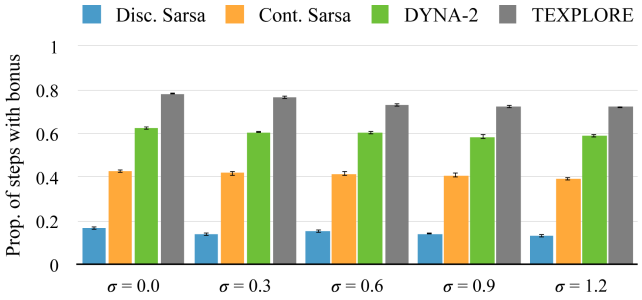

Fig. 5. Proportion of steps (out of 18000) in which the agents received a reward with a positive bonus. Results are groups by look-at distribution. Error bars represent standard errors. (Best viewed in color)

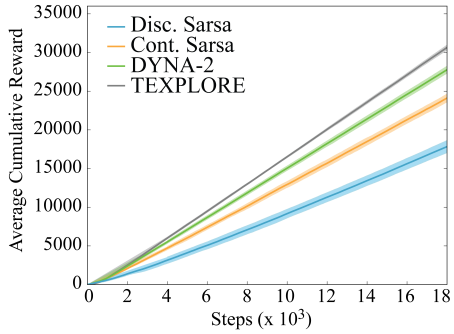

Fig. 6. Average cumulative reward for $\sigma = 0.0$. The shaded areas around the curves represent the standard error. Similar trends were obtained for the other look-at noise distributions. (Best viewed in color)

These findings are encouraging for future tests in real human-robot interactions because audio detection using microphone arrays tends to be more reliable than people detection with computer vision approaches. It is worth noting, though, that the wide field of view of the microphone array that we modeled for the robot and the lack of false positive detections likely influenced these outcomes.

C. Individual Behaviors

So far, we have considered situations in which the people in the conversation are all affected by the same look-at noise distribution and do not move. Of course, this not realistic.

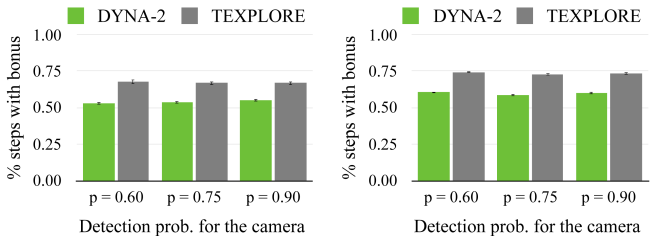

(a) Mic. detection prob. of 0.75 (b) Mic. detection prob. of 0.90

Fig. 7. Proportion of steps (out of 18000) in which the agents received a positive bonus as part of their reward. The left/right plots shows the results when the detection probability of the microphone array was 0.75/0.90.

People often exhibit individual behaviors that differentiate them from others. To study these types of situations, we investigated the performance of DYNA-2 and TEXPLORE when one person was affected by more look-at noise than the other people and when people slightly adjusted their position with respect to the rest of the group.

1) Non-Uniform Look-At Noise: For this test, we set the look-at noise distribution of one person to $\mathcal{N}(0, 1.2^2)$ and the rest to $\mathcal{N}(0, 0.6^2)$. Because there were four people in the simulation, we tested all four combinations with one outlier.

We found that the outlier look-at noise distribution did not affect the performance of the agents; the results were similar to those obtained for the experiment of Sec. VI-A. In particular, the proportions of steps in which the robot received a bonus reward were 0.58 (STE $<$ 0.01), 0.58 (STE $<$ 0.01), 0.59 (STE $=$ 0.01) and 0.59 (STE $=$ 0.01) with DYNA-2. With TEXPLORE, the proportions were 0.72 (STE $=$ 0.01), 0.73 (STE $<$ 0.01), 0.73 (STE $<$ 0.01), and 0.73 (STE $=$ 0.01). This result is not surprising given that the agents relied more on audio detections than visual information, as discussed in Sec. VI-B.

2) Changes in Location: We modified our simulation to induce small re-configurations of the people in the conversation. Every time a new speaker was selected, as described in Sec. III-B, we flipped a coin with a success probability p_t for every other person in the conversation. If the outcome of a flip was a success, we set a desired new position $\mathbf{p}'_i$ for the corresponding person i and updated his or her position towards this location at a constant velocity. In particular,

$$\mathbf{p}'_i = \begin{cases} \mathbf{p}_i + \mathbf{t}_i & \text{if } \|\mathbf{p}_i - \mathbf{p}_i^{ini}\| < 0.5 \text{ meters} \\ \mathbf{p}_i^{ini} & \text{otherwise} \end{cases} \quad (7)$$

with $\mathbf{p}_i^{ini}$ the initial location of person i at the beginning of the simulation, $\mathbf{p}_i$ their previous location, and $\mathbf{t}_i$ a translation drawn from a 2D normal distribution with mean $\mathbf{0}$ and covariance $[0.01\ 0.0; 0.0\ 0.01]$. In this manner, equation (7) induced controlled re-configurations of the spatial arrangement while preventing dissolving the group's F-formation.

For the test with translational motion, we considered four success probabilities p_t (0.1, 0.2, 0.3, and 0.4). In general, we used a constant look-at noise distribution of $\mathcal{N}(0, 0.6^2)$ and set the detection probabilities of the microphone array and the camera to 0.9 and 0.75, respectively.

Even though DYNA-2 and TEXPLORE learned good policies with translational motion, we found that this motion slightly reduced the learning speed of DYNA-2 in comparison to using $p_t = 0.0$ (as in Sec. VI-A). This outcome is illustrated in Figure 8. Each of the plots of this figure show the absolute angular difference between the robot and the direction towards the speaker from its location ($abs(\varphi)$ in eq. (2)). The baseline DYNA-2 (without translational motion) converged to an absolute offset of about 0.2 radians (11.5 degrees) after 12000 steps, whereas DYNA-2 took longer to converge with $p_t > 0.0$. TEXPLORE seemed to perform slightly better with translational motions, likely because its policy was better suited for our problem.

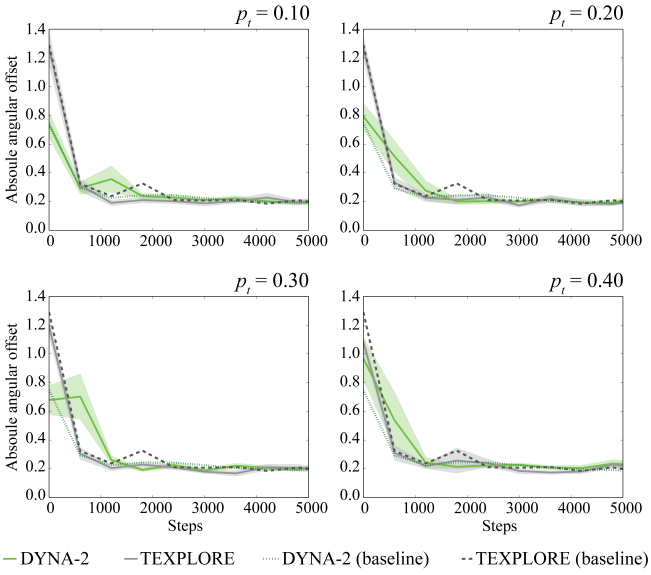

Fig. 8. Absolute angular offset (in radians) between the robot's direction and the direction towards the speaker. Results were averaged over windows of 600 contiguous steps and over 10 runs for each agent. The shaded areas behind the DYNA-2 and TEXPLORE lines represent std. errors. Baseline results correspond to $p_t = 0.0$, i.e., no translational motion. (Best viewed in color)

D. Generalization To Other Groups

Finally, we decided to test how well pre-trained agents performed in other conversations with different numbers of people. For this test, we exposed the DYNA-2 and TEXPLORE agents that were trained with 4 people for the experiment of Sec. VI-A to interactions with 2, 3, 5 and 6 people. For interactions with less than 4 people, we used a stride of 1.25 meters, as in the other experiments. When more people conversed with the robot, we increased the stride to 1.5 meters to accommodate the extra participants. For this experiment, we also let the agents adjust their Q value estimates in an online fashion. Each run lasted a total of 3000 steps (10 minutes of interaction time).

Figure 9 shows the average number of steps for which the agents received a bonus reward in the new environment. As expected, the agents that were pre-trained outperformed agents that started to learn from scratch. This result shows the generalization power of our state representation.

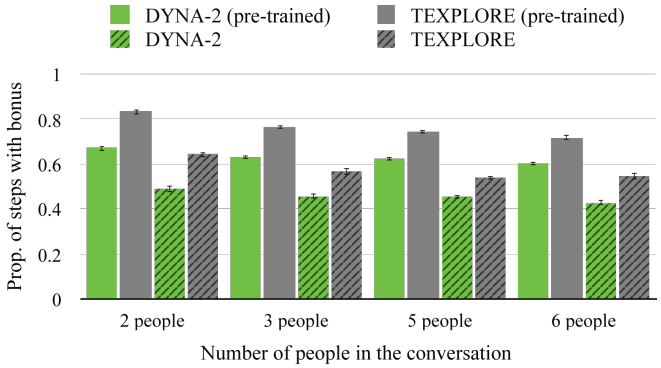

Fig. 9. Proportion of steps (out of 3000) in which the robot got a reward with a positive bonus. Pre-trained agents interacted with 4 people prior to this test; other agents learned from scratch. Error bars represent std. errors.

VII. DISCUSSION

We explored reinforcement learning methods to control the orientation of a robot during simulated multi-party conversations. Our main assumption throughout this work was that the robot should turn towards the speaker to convey attentiveness and maintain awareness of the focus of attention.

The state representation that we designed for the RL task encodes the likely direction of the speaker from the perspective of the robot, as captured by a camera and a microphone array on the platform. This representation is agnostic to the number of people in the conversation and, thus, can be used to generalize learned behaviors across social contexts.

Limitations. Our simulated environment was inspired by models from social psychology that describe spatial behavior during group interactions, but did not fully capture all the complexity of real world conversations nor sensing noise. For example, only one person spoke at a time in the simulation, even though people sometimes speak simultaneously during conversations. Furthermore, the sensors that we simulated either detected people correctly or didn't detect them at all. Real sensors, however, typically provide detection scores and suffer from false positive detections.

Implications & Future Work. Our findings suggest that RL has potential to succeed in motion control tasks during social conversations. In comparison to manually designing a policy to control the orientation of a robot, RL methods tend to scale more easily as the dimensionality of the state space increases. That is, RL methods can incorporate more easily additional aspects of the interaction in the decision making process. As we move forward towards controlling a real platform, this increase in dimensionality will likely be necessary to deal with the added complexity of real interactions. For example, we expect that using the detection probability of the microphone array in the state representation, rather than using a binary feature for whether or not a detection was successful, would lead to more robust policies. Similarly, incorporating a score for how many people gaze towards the point of maximum social saliency would help identify important social saliency locations from minor foci of attention. Of course, we pay a price for this flexibility: RL methods need data to learn from. To reduce the amount of data that we will need to train a robot in real life, we plan to improve our simulation and use the policies learned from it as prior knowledge. We expect this prior to reduce the time needed to learn good policies in practice.

ACKNOWLEDGMENTS

We thank Disney Research for continued support of this research effort, as well as Christoph Dann and Emma Brunskill for their feedback and suggestions.

REFERENCES

[1] M. M. Veloso, J. Biswas, B. Coltin, and S. Rosenthal, "CoBots: Robust Symbiotic Autonomous Mobile Service Robots," in *IJCAI'15*, 2015.
[2] V. Evers, N. Menezes, L. Merino, D. Gavrila, F. Nabais, M. Pantic, P. Alvito, and D. Karreman, "The Development and Real-world Deployment of FROG, the Fun Robotic Outdoor Guide," in *HRI'14*, 2014.
[3] M. Vázquez, A. Steinfeld, S. E. Hudson, and J. Forlizzi, "Spatial and Other Social Engagement Cues in a Child-robot Interaction: Effects of a Sidekick," in *HRI'14*, 2014.
[4] J. Vroon, M. Joosse, M. Lohse, J. Kolkmeier, J. Kim, K. Truong, G. Englebienne, D. Heylen, and V. Evers, "Dynamics of social positioning patterns in group-robot interactions," in *RO-MAN'15*, 2015.
[5] D. E. Karreman, G. D. Ludden, E. M. van Dijk, and V. Evers, "How can a tour guide robot's orientation influence visitors' orientation and formations?" in *Int'l Symp. on New Frontiers in HRI*, 2015.
[6] M. A. Yousuf, Y. Kobayashi, Y. Kuno, A. Yamazaki, and K. Yamazaki, "Development of a Mobile Museum Guide Robot That Can Configure Spatial Formation with Visitors," in *Intelligent Computing Technology*, ser. Lecture Notes in Computer Science, 2012, vol. 7389, pp. 423–432.
[7] R. Mead and M. J. Matarić, "Perceptual models of human-robot proxemics," in *ISER'14*, 2014.
[8] J. Kober, J. A. Bagnell, and J. Peters, "Reinforcement Learning in Robotics: A Survey," *The Int'l J. of Robotics Research*, 2013.
[9] M. Saerbeck and C. Bartneck, "Perception of Affect Elicited by Robot Motion," in *HRI'10*, 2010.
[10] H. Kuzuoka, Y. Suzuki, J. Yamashita, and K. Yamazaki, "Reconfiguring Spatial Formation Arrangement by Robot Body Orientation," in *HRI'10*, 2010.
[11] A. Steinfeld, O. C. Jenkins, and B. Scassellati, "The Oz of Wizard: Simulating the human for interaction research," in *HRI'09*, 2009.
[12] R. S. Sutton and A. G. Barto, *"Reinforcement Learning: An Introduction"*. The MIT Press, 2015, (second edition, in progress).
[13] E. Goffman, *Behavior in public places: Notes on the social organization of gatherings*. Free Press of Glencoe, 1963.
[14] A. Kendon, *Conducting Interaction: Patterns of Behavior in Focused Encounters*. Cambridge Univ. Press, 1990.
[15] H. S. Park, E. Jain, and Y. Sheikh, "3D Social Saliency from Head-Mounted Cameras," in *NIPS'12*, 2012.
[16] F. Setti, C. Russell, C. Bassetti, and M. Cristani, "F-formation Detection: Individuating Free-standing Conversational Groups in Images," *CoRR*, vol. abs/1409.2702, 2014.
[17] M. Vázquez, A. Steinfeld, and S. E. Hudson, "Parallel Detection of Conversational Groups of Free-Standing People and Tracking of their Lower-Body Orientation," in *IROS'15*, 2015.
[18] T. Hester, "TEXPLORE: Temporal Difference Reinforcement Learning for Robots and Time-Constrained Domains," Ph.D. dissertation, The University of Texas at Austin, Texas, USA, December 2012.
[19] D. Silver, R. S. Sutton, and M. Müller, "Temporal-difference search in computer Go," *Machine Learning*, vol. 87, no. 2, pp. 183–219, 2012.
[20] R. S. Sutton, "Temporal Credit Assignment in Reinforcement Learning," Ph.D. dissertation, University of Massachusetts Amherst, 1984.
[21] Richard S. Sutton, "Generalization in reinforcement learning: Successful examples using sparse coarse coding," *Advances in Neural Information Processing Systems*, pp. 1038–1044, 1996.
[22] R. S. Sutton, "Tile Coding Software," http://rlai.cs.ualberta.ca/RLAI/RLtoolkit/tiles.html, Online; accessed Feb. 2016.
[23] W. Dabney and A. Barto, "Adaptive Step-Size for Online Temporal Difference Learning," in *AAAI'12*, 2012.
[24] L. Kocsis and C. Szepesvári, "Bandit Based Monte-Carlo Planning," in *ECML'06*, 2006.